

This is the final peer-reviewed accepted manuscript of:

Ragazzini I., Gualandi I., Selli S., Polizzi C., Cassani M.C., Nanni D., Gambassi F., Tarterini F., Tonelli D., Scavetta E., Ballarin B. "A simple and industrially scalable method for making a PANI-modified cellulose touch sensor", in Carbohydrate Polymers, 2021, 254

The final published version is available online at:
<https://doi.org/10.1016/j.carbpol.2020.117304>

Terms of use:

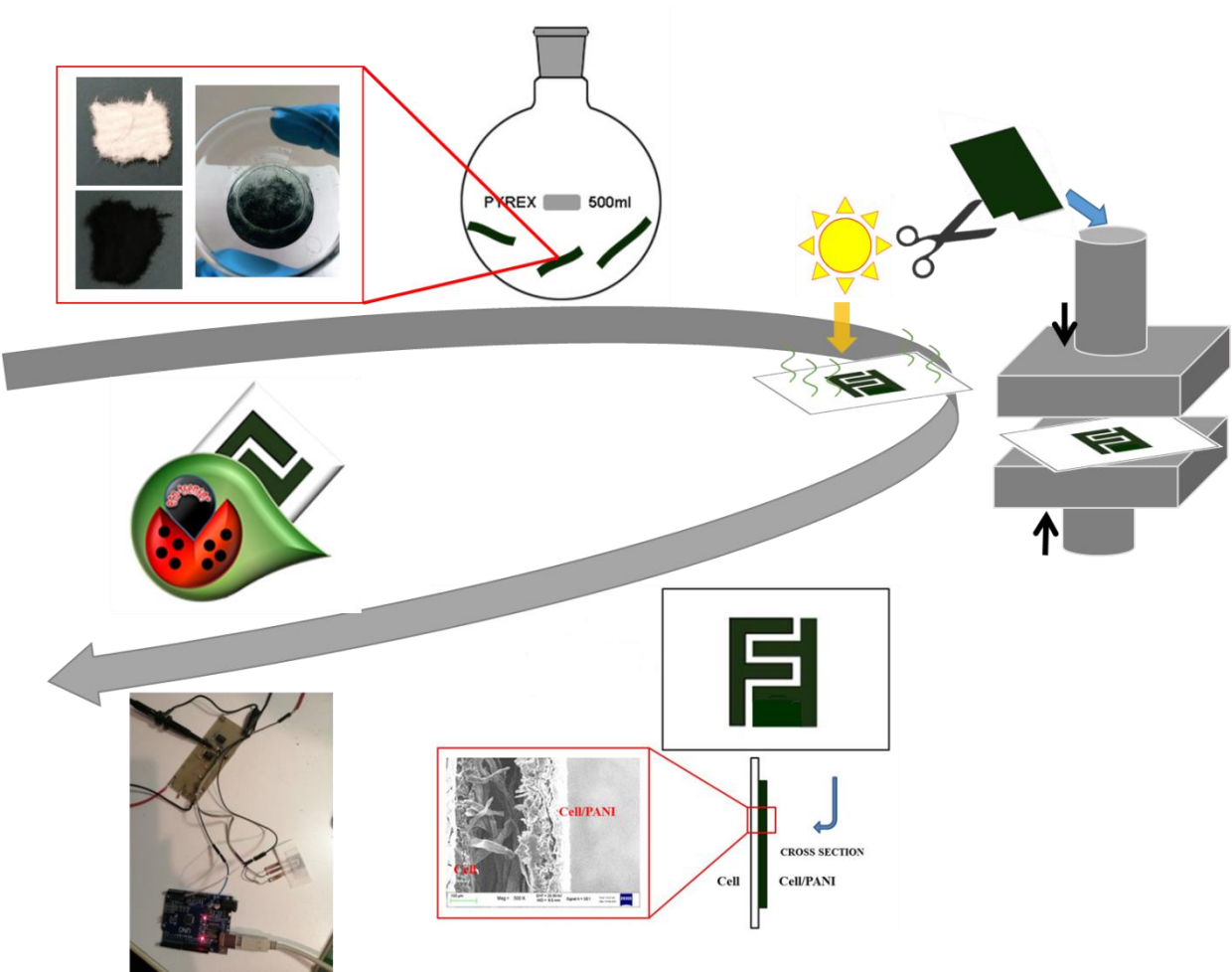
Some rights reserved. The terms and conditions for the reuse of this version of the manuscript are specified in the publishing policy. For all terms of use and more information see the publisher's website.

This item was downloaded from IRIS Università di Bologna (<https://cris.unibo.it/>)

When citing, please refer to the published version.

19 **Graphical abstract**

20



21

22

A simple and industrially scalable method for making a PANI-modified cellulose touch sensor

I. Ragazzini^a, I. Gualandi^{a*}, S. Selli^b, C. Polizzi^a, M. C. Cassani^a, D. Nanni^a, F. Gambassi^a, D. Tonelli^a,
E. Scavetta^a, B. Ballarin^{a*}

^aDepartment of Industrial Chemistry “Toso Montanari”, Bologna University, Via Risorgimento 4, I-40136, Bologna, Italy.

^bCromatos s.r.l., via G. Cardano, 6B/C/D – 47122 Forlì, Italy.

*To whom correspondence should be addressed. E-mail: barbara.ballarin@unibo.it (B.B), tel: +39 051 2093700; isacco.gualandi2@unibo.it (I.G.), tel: +39 051 2093386.

Abstract

In this work we present a simple, inexpensive, and easily scalable industrial paper process to prepare sheets of conductive cellulose fibers coated with polyanilines. First, bare fibers were coated by in situ oxidative polymerization of polyaniline then, the resulting composite fibers were used to fabricate electroactive sheets. The resistivity of the sheets is $14 \pm 1 \Omega \text{ sq}^{-1}$, a value around 1000 times lower than those reported in literature. The superior electronic proprieties of the sheets were demonstrated by assembling a capacitive touch sensor device with optimized geometry. The touch sensor shows an increase of 3-4 % of the starting electric capacity after compression and a fast response time of 52 ms. To our knowledge this is the first time that a device is prepared in this way and therefore, the herein presented results can bring an significant improvement in the development of low-cost, green and high-tech electronic devices.

Keywords: electro-active paper; PANI; cellulose; transducers; touch sensor

1. INTRODUCTION

In the current world, many action is eased by the presence of electrical devices but only 20% of these appliances is correctly recycled. Many landfills continue to be stuffed with unwanted electronics and workers are exposed to hazardous and carcinogenic substances during informally recycling processes in developing countries. As new products are consumed by hungry customers wanting the latest and greatest technology, the sheer volume of these daily produced discarded materials makes this task apparently insurmountable (EU Report).

Research efforts are focused on the development of an alternative to traditional electronics that should be low-cost, degradable, compostable, and made from environmentally nontoxic substances. As a candidate, cellulose is one of the most investigated raw materials, mainly because of high abundance on Earth, biocompatibility, porosity, high flexibility and light-weight (Khan, Abas, Kim, & Kim, 2016) (Luo & Huang, 2014). In addition, its low price (about 0.1 cent dm⁻²) (Tobjörk & Österbacka, 2011) and its recyclability make cellulose an economically very viable option (John, Mahadeva, & Kim, 2010) (Kanaparthi & Badhulika, 2017) (Tian, Qu, & Zeng, 2017). Despite its high surface resistivity at relative humidity of 20-40 % (typically 10¹¹-10¹⁵ Ω sq⁻¹) (Tobjörk & Österbacka, 2011), it can be used as support to produce conductive paper that can be exploited in a wide range of applications, including supercapacitors, microfluidic systems, diagnostic devices, actuators and sensors (Luo & Huang, 2014) (Kanaparthi & Badhulika, 2017) (Sanandiya, Vijay, Dimopoulou, Dritsas, & Fernandez, 2018) (Q. Wang et al., 2018).

Two different approaches to prepare conductive paper are described in literature. In the first one, organic or inorganic conductive, semi-conductive and dielectric printable materials is deposited on paper employing screen, inkjet printing or flexographic techniques (Tobjörk & Österbacka, 2011). The second approach consists in embedding conductive materials such as functionalized multi-walled carbon nanotubes, inorganic nanoparticles and conducting polymers (CPs) in cellulose fibers making them conductive (Khan et al., 2016) (Tobjörk & Österbacka, 2011) (John et al., 2010) (Yan et al.,

2016) (Pang et al., 2016) (Gu & Huang, 2013) (Rafatmah & Hemmateenejad, 2020) (Das, Mai, & Duan, 2019) (Y. Zhang et al., 2019) (Silva et al., 2019) (Sharma, Pareek, Rohan, & Kumar, 2019) (W. Zhang et al., 2019) (Zang et al., 2018). Conducting cellulosic fibers produced by coating with CPs (i.e. polyaniline (PANI), polypyrrole (PPY), poly(3,4-ethylenedioxythiophene) (PEDOT) etc.) are being explored for various applications including supercapacitors, batteries, transistors, conductive wires, actuators and touch sensors (Tobjörk & Österbacka, 2011) (Aguado, Murtinho, & Valente, 2019) (Ma, Wang, & Yu, 2020).

In this scenario PANI is particularly interesting because of its low cost, easy preparation, good environmental stability and tunable electrical properties by varying its oxidation state (Tobjörk & Österbacka, 2011)(Singh & Shukla, 2020)(Yanmin Wang, Liu, Han, & Li, 2019)(Tanguy, Thompson, & Yan, 2018)(Yanmin Wang et al., 2019)(Shoaie et al., 2019). In situ polymerization is the most popular way of depositing PANI on cellulosic fibers. Different methods can be employed depending on the types of fiber, oxidants, medium, dopants, monomers, concentration used, processing steps and parameters (John et al., 2010) (Ma et al., 2020) (Singh & Shukla, 2020) (Ke et al., 2019).

Herein we first report the preparation of cellulose/PANI fibers (Cell/PANI-F) in which PANI, in the form of protonated conductive emeraldine salt, was obtained by a simple in situ oxidative polymerization of aniline on bare cellulose fibers in acidic media (Ma et al., 2020) (Ke et al., 2019) (Masood et al., 2019). Successively, the fibers were assembled to give electroactive sheets (Cell/PANI-S) with different thickness and resistivity: 1.25 mm with a resistivity of $14 \pm 1 \Omega \text{ sq}^{-1}$ (0.5 S cm^{-1}) or 0.4 mm with a resistivity of $237 \pm 9 \Omega \text{ sq}^{-1}$ (0.1 S cm^{-1}). Finally, differently from those reported in the literature which are normally of resistive type (Tao et al., 2017) (Shao et al., 2014), capacitive touch sensors (Cell/PANI-TS) with an optimized geometry were assembled. Both electroactive sheets and touch sensors were prepared using an industrially and easily scalable paper process provided by the industrial group Cromatos s.r.l. (<https://www.cromatos.com>).

The capacitive touch sensors were finally interfaced with Arduino UNO developed board to investigate their dynamic response. All the measures have been conducted at room temperature and

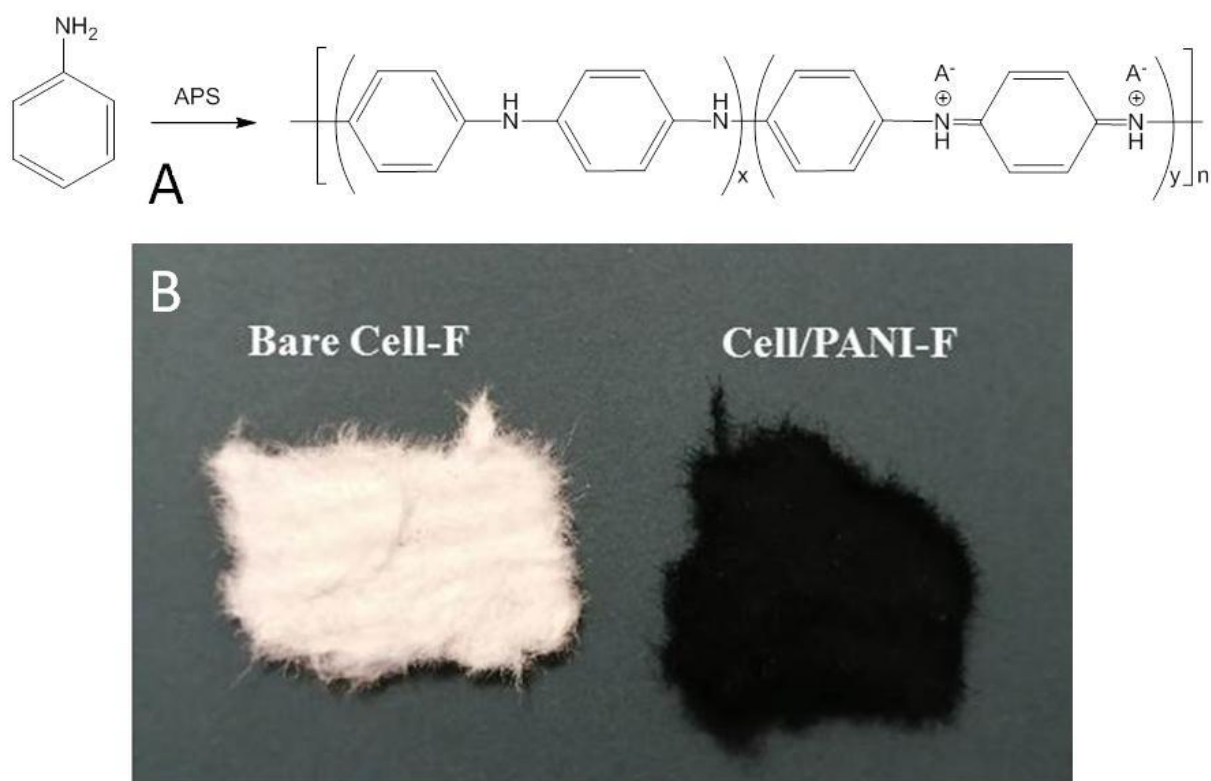
99 in natural environment humidity after that the Cell/PANI-S or the Cell/PANI-TS were subjected to
100 air at room temperature for the time of 24 h.

101

102 2. RESULTS AND DISCUSSION

103 2.1. Preparation and characterization of Cell/PANI-F and Cell/PANI-S

104 The modification of bare cellulosic fibers with PANI was obtained via a simple in situ oxidative
105 polymerization of aniline in acid media, as described in the experimental section (Fig. 1).

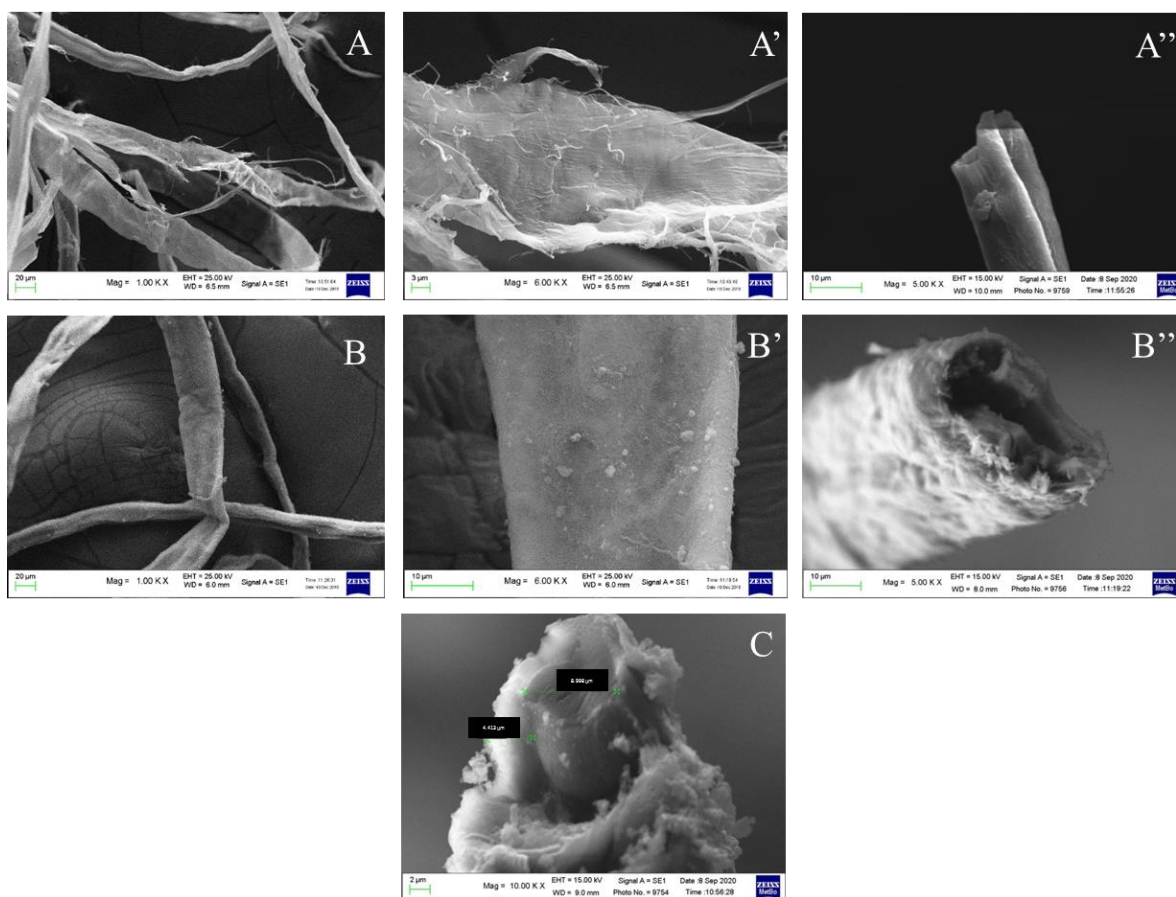


106

107 **Fig. 1.** A) Schematic representation of the oxidative polymerization of aniline with ammonium
108 persulfate $[(\text{NH}_4)_2\text{S}_2\text{O}_8, \text{APS}]$ in acid media; B) Image of Bare Cell-F (white) and Cell/PANI-F
109 (black) after filtration and drying.

110

111 Scanning electron microscopy (SEM) images of bare cellulose fibers and Cell/PANI-F are
112 reported in Fig. 2.



113

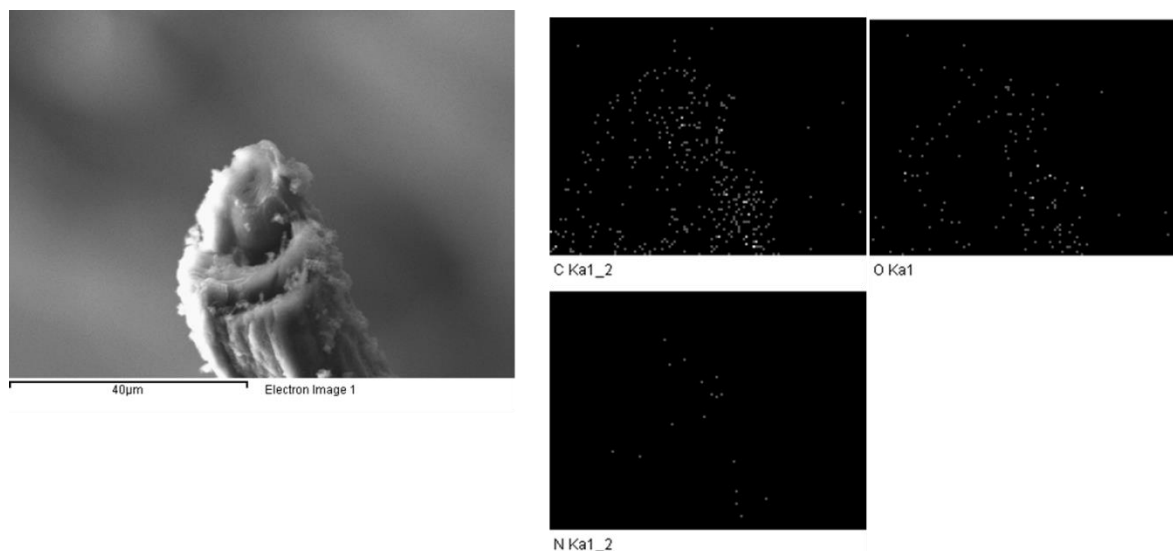
114 **Fig. 2.** Scanning electron microscopy (SEM) of bare Cell-F (A, A', A'') and Cell/PANI-F (B, B',
 115 B'') at 1000 X, 6000 X and 5000 X magnification, respectively; C) Cross-section of Cell/PANI-F at
 116 10000 X magnification.

117 It can be seen from the SEM images that the pure Cell-F (Figs. 2A-A'') displayed a very clean and
 118 smooth morphology, whereas the Cell/PANI-F displayed relatively rough surface (Figs. 2B-B'').
 119 Compared the surface morphology the Cell/PANI-F is significantly different due to the deposition of
 120 PANI on the surface. All the cellulose surface results covered by a rough film that is ascribed to
 121 PANI. The PANI layer showed a relative compact morphology and well wrapped the cellulose fibers
 122 with a thickness around 4.4 μm, as observable in Fig. 2C.

123 SEM image and EDS element mappings of Cell/PANI-F sample are presented in Fig. 3. Within the
 124 elemental maps, the C signal originates from the cellulose fiber and PANI; O signal comes from

cellulose fiber and the N signals uniquely indicate the PANI regions. N was observed only in the outer space of cellulose fibers.

127



128

129 **Fig. 3.** EDS elemental mapping of CELL/PANI-F for Carbon, Oxygen and Nitrogen.

130

131 The PANI average amount on cellulose fibers was measured using the Kjeldahl method after
132 digestion of the Cell/PANI-F sample and resulted 22.3 wt%.

133 The conductive sheets Cell/PANI-S were prepared from the Cell/PANI-F, using a protocol
134 commonly employed for coloring paper with acid dyes (Supplementary Information, SI and Scheme
135 S1) (Cartari, 2003). In order to maintain the polyaniline in the oxidized state (emeraldine salt), the
136 modified fibers were immersed in a 25% $\text{Al}_2(\text{SO}_4)_3$ aqueous solution kept at *ca.* pH 3.0. Successively,
137 after being partially dried in a square sieve and kept in a press at 50 bar for 10 s, sheets of 200 grams
138 for square meter (200 gsm) and a thickness of 0.40 mm were obtained. Alternatively, thicker sheets
139 (1.25 mm; 630 gsm) were prepared in a similar fashion.

140 The ATR-FTIR spectra of Cell/PANI-S (Fig. 4) show all the characteristic peaks attributed to
141 PANI: the stretching vibrations of benzoid N-B-N and quinoid N=Q=N structures show up at 1443
142 and 1564 cm^{-1} , separately. The absorption band at 1290 is ascribed to protonation of PANI. Bare

cellulose shows the characteristic absorption peaks at ca. 3300 cm^{-1} attributed to the stretching of hydroxyl groups $\nu(-\text{OH})$ and 2900 cm^{-1} attributed to the stretching of C-H groups; moreover, in the region of 1300 cm^{-1} the -OH bending and the C-O antisymmetric bridge stretching are present and the strong bands around 1000 cm^{-1} due to the C-O-C pyranose ring skeletal vibration are observed (Chougale, Thombare, Fulari, & Kadam, 2013) (Cases, Huerta, Garcés, Morallón, & Vázquez, 2001) (Liu et al., 2005) (Dhibar & Das, 2014).

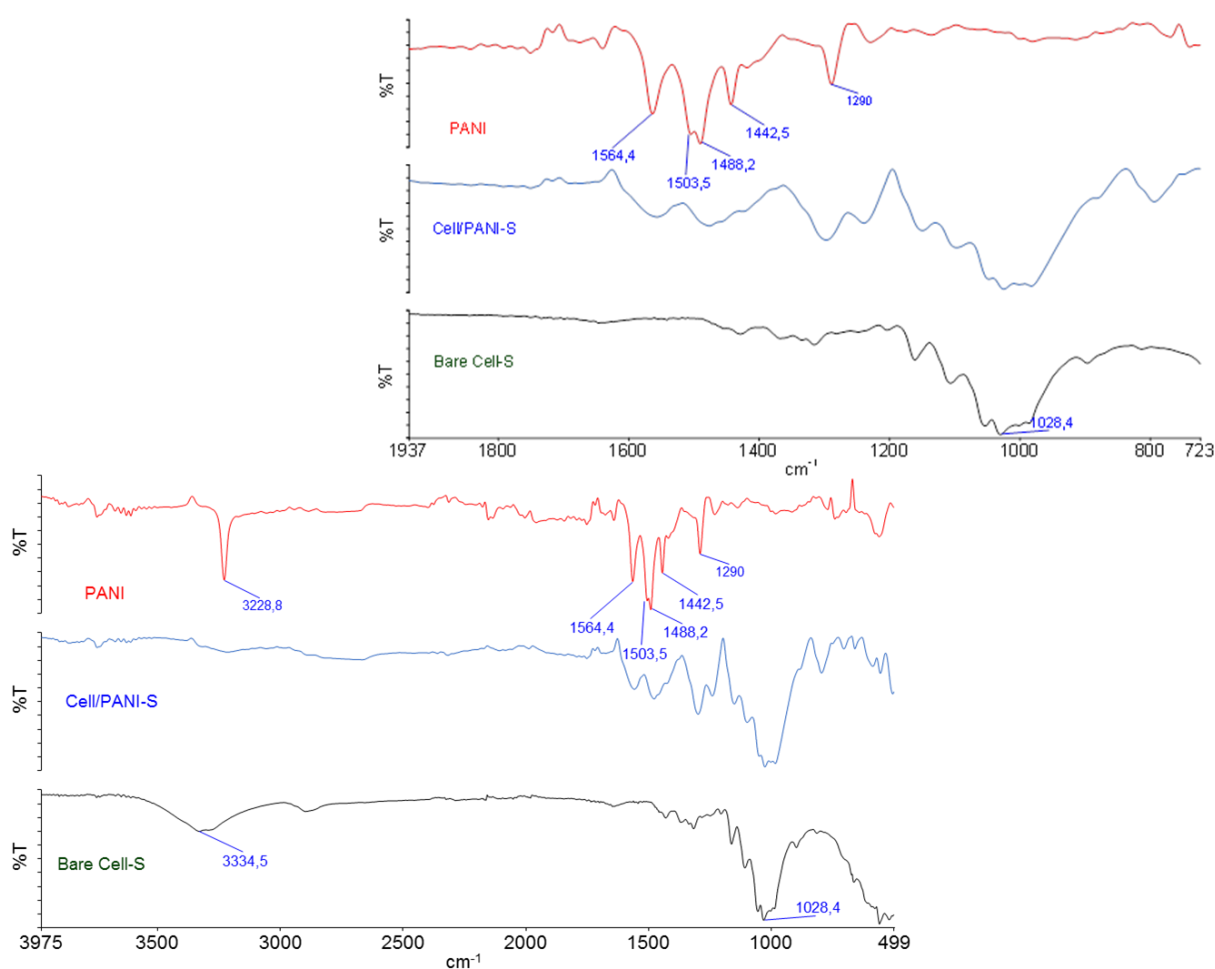


Fig. 4. ATR-FTIR spectra of bare Cellulose (black), PANI (red) and Cell/PANI-S (blue); inset: enlargement in the range $1900\text{--}700\text{ cm}^{-1}$.

2.2 Cell/PANI-S electrical features

154 The Cell/PANI-S conductivity was evaluated by 4-line-probe measurements with a home-made
 155 sample holder (Fig. S2) to avoid the contribution due to contact resistances. In order to evaluate the
 156 reproducibility of the system, the effect of different morphology and the influence of the
 157 environmental condition during the real use, the electrical characterization was performed at different
 158 times, for each thickness, on three different paper sheets at room temperature and balanced with the
 159 surrounding atmosphere. As expected, it was found that the conductivity of Cell/PANI-S depends on
 160 the sheet thickness being $0.105 \pm 0.004 \text{ S cm}^{-1}$ for a thickness of 0.40 mm and $0.56 \pm 0.06 \text{ S cm}^{-1}$ for
 161 a thickness of 1.25 mm; in the latter the value is only one order of magnitude lower than the highest
 162 values reported for pristine PANI. It is important to underline that our preparation method allows to
 163 obtain conductivity values higher (or similar, depending from the thickness) than those achievable by
 164 all the conductive papers presented in literature, as evident from the data reported in Table 1. The
 165 small standard deviation obtained suggested the low influence of the external environmental variation
 166 (i.e. humidity).

167 **Table 1.** Comparison of the conductivity of different samples based on PANI.

Material	Synthesis	Conductivity (S cm^{-1})	Ref.
Cell/PANI-S	In situ synthesis on the cellulose pulp (1.25 mm thickness)	$5.6 \pm 0.6 \cdot 10^{-1}$	This work
Cell/PANI-S	In situ synthesis on the cellulose pulp (0.4 mm thickness)	$1.05 \pm 0.04 \cdot 10^{-1}$	This work
Rice pulp/PANI	In situ synthesis on the cellulose pulp	$2.5 \cdot 10^{-5}$	(Youssef, El-Samahy, & Abdel Rehim, 2012)
Pineapple fibers/PANI	In situ synthesis on the cellulose pulp	$3.0 \cdot 10^{-4}$	(S. I. A. Razak, N. F. A. Sharif, 2014)
Cellulose pulp/PANI	In situ synthesis on the cellulose pulp. Chemimetric optimization	$1.5 \cdot 10^{-2}$	(Sharifi, Zabihzadeh, & Ghorbani, 2018)
CA electrospun/PANI	In situ polymerization onto electrospun cellulose membrane	$1.0 \cdot 10^{-1}$	(Baptista et al., 2018))
Cellulose/PANI	Dispersed Cellulose + PANI	$4.7 \cdot 10^{-8}$	(John et al., 2010)
Ink-jet printed PANI	Ink composed by PANI nanoparticles	$4.0 \cdot 10^{-4}$	(Ngamna et al., 2007)

Thin PANI film on filter paper	In situ polymerization on masked paper sheet	$1.0 \cdot 10^{-3}$	(Gao, Ota, Kiriya, Takei, & Javey, 2019)
PANI bulk		1-5	(Teo et al., 2019)

In order to clearly demonstrate the excellent conductivity of Cell/PANI-S, two 1.25 mm thick paper sheets were successfully used as wires to transport the current necessary to power a LED with an applied voltage of 2.0 V (Fig. 5).

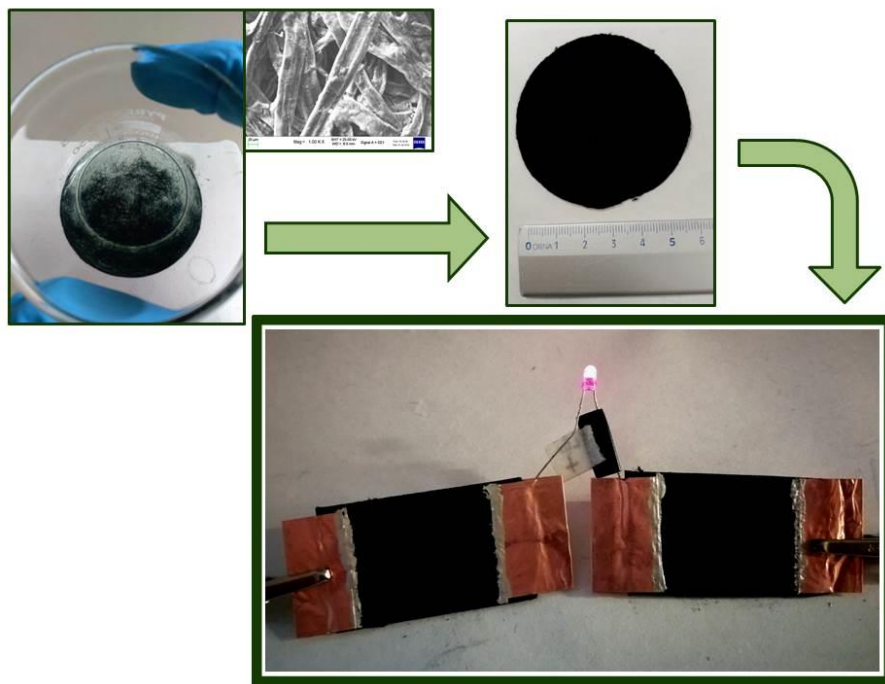


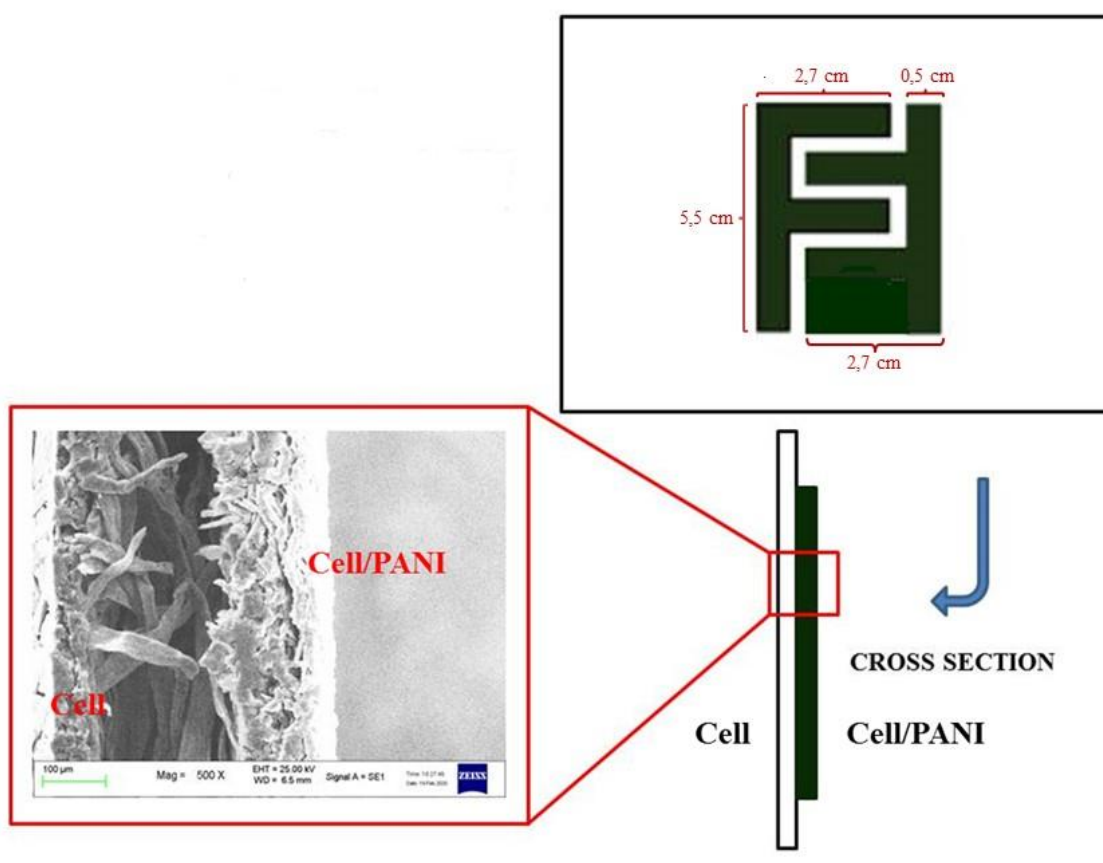
Fig. 5. Experimental setup with Cell/PANI-S (1.25 mm) and LED.

2.3 Cell/PANI-TS assembling and performance

Cell/PANI-TS was prepared by an industrial assembling method coupling a Cell/PANI-S (0.4 mm, 200 gsm) suitably cut with scissors in the required shape and a cellulose sheet (0.4 mm, 200 gsm), as described in the experimental section. By maintaining the composite under a 50 bar pressure for 10

179 s, a device with a thickness of 0.80 mm has been obtained as reported in Figure 6 and Scheme S2.
 180 Dimensions and shape of the built circuit can be easily varied as reported in Fig. S3.

181



182

183 **Fig. 6.** Cell/PANI-TS: SEM image of the cross section and assembled circuit.

184

185 To understand the functionality of the capacitive touch sensor, an experimental test has been
 186 set up using a home-made equipment which allows to exercise and control the pressure given on the
 187 touch sensor with a step by step motor. The pressure was applied by keeping the position unchanged,
 188 and the whole area of the touch sensor was stimulated. Then the force-weight at each single advance
 189 step of the motor was measured and the capacity was recorded at the same time with Arduino UNO
 190 board (see Figs. S4-S8 and Scheme S3 for details).

Three Cell/PANI-TS samples with different geometries were tested (Fig. 7). For each, the capacitive component was measured without any touch interaction and during the dynamically induced increasing pressure up to a maximum value of 22 kPa (saturation level). The Cell/PANI-TS was excited by a square wave through the Weight Force Generator (WFG) while the out-put signal was observed with the oscilloscope and acquired with Arduino UNO development board, as described in SI. All three touch sensors have a starting capacity of about 93-94 pF and different saturation capacity depending on the geometry employed, however an increase of 3-4 % of the initial value after pressure exertion is always obtained. Fig. 7 shows the results of the tests reporting $\Delta C/C_0$ % vs pressure, where ΔC is $(C_P - C_0)$, C_P and C_0 correspond to the capacity with and without pressure (Zang et al., 2018) (Tao et al., 2017) (Yu, Tang, Cai, Ren, & Tang, 2019) (Cataldi et al., 2018).

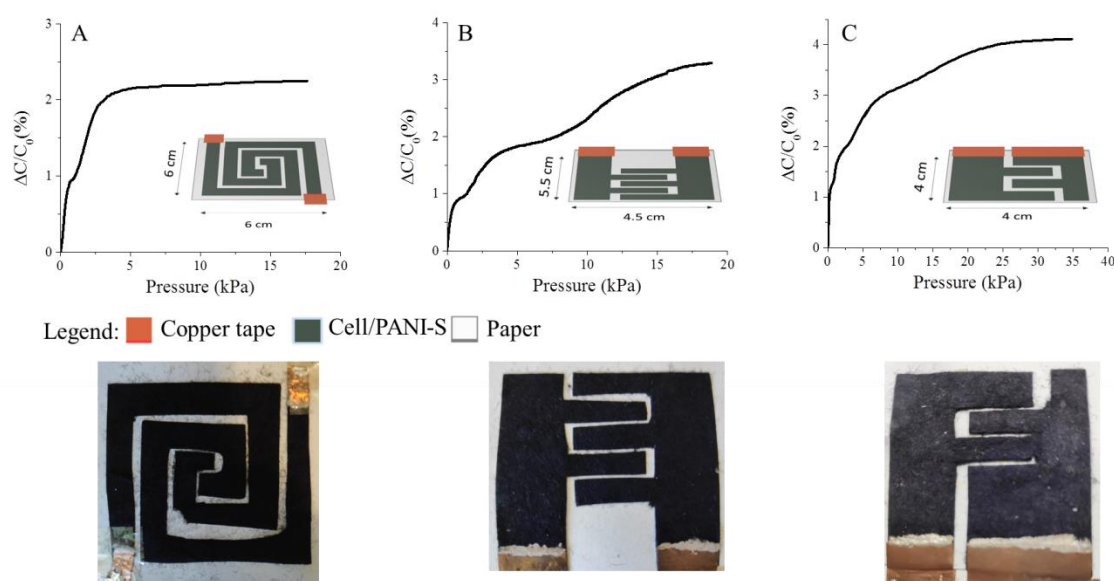


Fig. 7. Cell/PANI-TS with different geometry and related change of capacity with pressure curves.

From the data comparison, it can be observed that the geometry heavily affects the response as shown in Fig. 7. A-type sensor shows two different linear trends with a sensitivity, defined by $(C_P - C_0)/C_0/P$ where P is the used pressure (Zang et al., 2018) (Tao et al., 2017) (Yu et al., 2019), of 0.66 kPa^{-1} in a small pressure range (0 to 2 kPa) and 0.012 kPa^{-1} in a large pressure range (2 to 20 kPa) (Figure S9). On the contrary, the C-type sensor curve follows a logarithmic trend with equation $y =$

209 $0.598 \ln(x) + 1.724$; $R^2 = 0.954$ (Fig. S10) and shows sensitivities of 2.34 (0.45 $\sigma\%$), 1.37 (0.44 $\sigma\%$)
210 and 0.19 (0.44 $\sigma\%$) kPa^{-1} at pressures of 0.5, 2 and 20 kPa, respectively (average of five different
211 measurements). Under each pressure both sensors display a good and stable response. Finally, B-type
212 sensor present a different behavior which cannot be traced back to a simple mathematical expression.
213 Due to its logarithmic behavior, we have chosen to carry out the repeatability and stability tests only
214 on C-type sensors, recording, for each device, six independent $\Delta C/C_0$ % vs pressure curves, at
215 different data. The results shown in Fig. S11, indicate a good reproducibility under all pressure range
216 without a noticeable degradation of the performances.

217 Finally, a pressure around 6 kPa was used to examine the sensors time response revealing a
218 response time of 52 ± 1 ms.

219

220 3. CONCLUSIONS

221 To the best of our knowledge, for the first time, an easily scalable industrial paper process is here
222 proposed to produce conductive paper sheets with excellent electrical performances as demonstrated
223 by the success of their use in the fabrication of capacitive touch sensors. This method can provide an
224 enormous improvement in the field of low-cost electronic technology. The electroactive sheets exhibit
225 a conductivity around five times higher than those reported in literature for similar systems and can
226 be employed to light a LED with an applied potential of 2.0 V, highlighting the outstanding electrical
227 performances of these composite materials. The capacitive touch sensors show a very quick response
228 time (52 ms) and a sensibility that can be easily modulated by changing the geometry of the device.

229

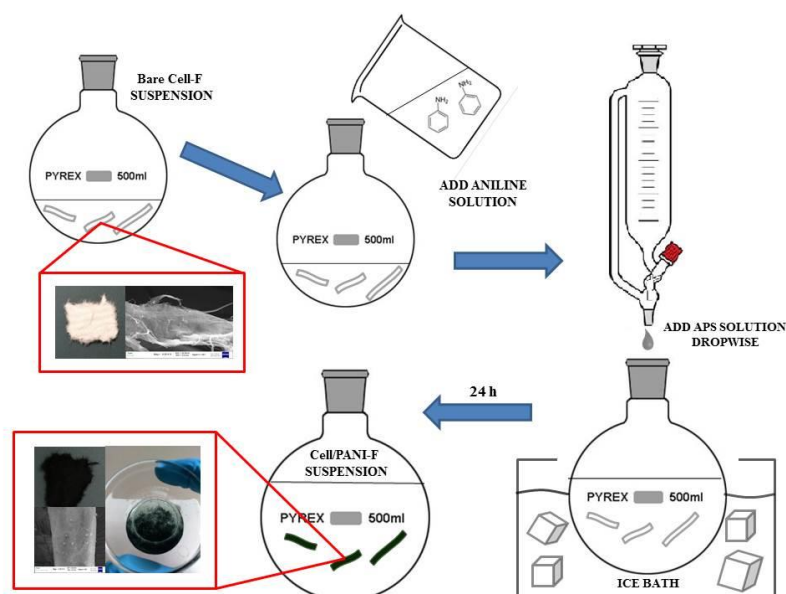
230 4. EXPERIMENTAL SECTION

231 4.1 Materials

232 All chemicals and solvents are ACS reagent grade, were purchased from commercial vendors and
 233 used directly unless otherwise stated. Sulfuric acid (H_2SO_4 , 95.0-98.0%), ammonium persulfate
 234 $[(\text{NH}_4)_2\text{S}_2\text{O}_8]$, $\geq 98\%$ and aniline ($\geq 99\%$), were purchased from Sigma-Aldrich (now Merck KGaA,
 235 Darmstadt, Germany); aniline was distilled under nitrogen prior to use. Citric acid ($\geq 99.5\%$) was
 236 purchased from VWR Chemicals (Vienna, Austria); a solution of ca. 25 wt% of $\text{Al}_2(\text{SO}_4)_3$ in water
 237 (commercial name FLOCLINE S8C) was purchased from Bio-Line s.r.l. (Milano, Italy). Bare
 238 cellulose fibers (pine tree long fiber with sulfate treatment) were kindly provided by Cromatos s.r.l.
 239 (Forlì, Italy).

240 4.2 Preparation of Cell/PANI-F

241 In a 1 L round bottom flask, 2.5 g of bare cellulose fibers were dispersed in demineralized water (250
 242 mL) for 30 min; successively a solution made of 2.5 mL of aniline in 150 mL of 1.0 M citric acid
 243 ($\text{C}_6\text{H}_8\text{O}_7$) was added to the fiber suspension and stirred for 3 h at room temperature. In turn, the
 244 oxidative polymerization was carried out adding dropwise to the stirred suspension, previously cooled
 245 to 0 °C in an ice bath, a solution of 7 g of $(\text{NH}_4)_2\text{S}_2\text{O}_8$ dissolved in 200 mL of 1.0 M citric acid. After
 246 24 h the coated fibers were filtered in a Buchner funnel and washed several times with 1.0 M citric
 247 acid solution. The conductive fibers were dried in air atmosphere for 24 h; see Scheme 1 for details.



248

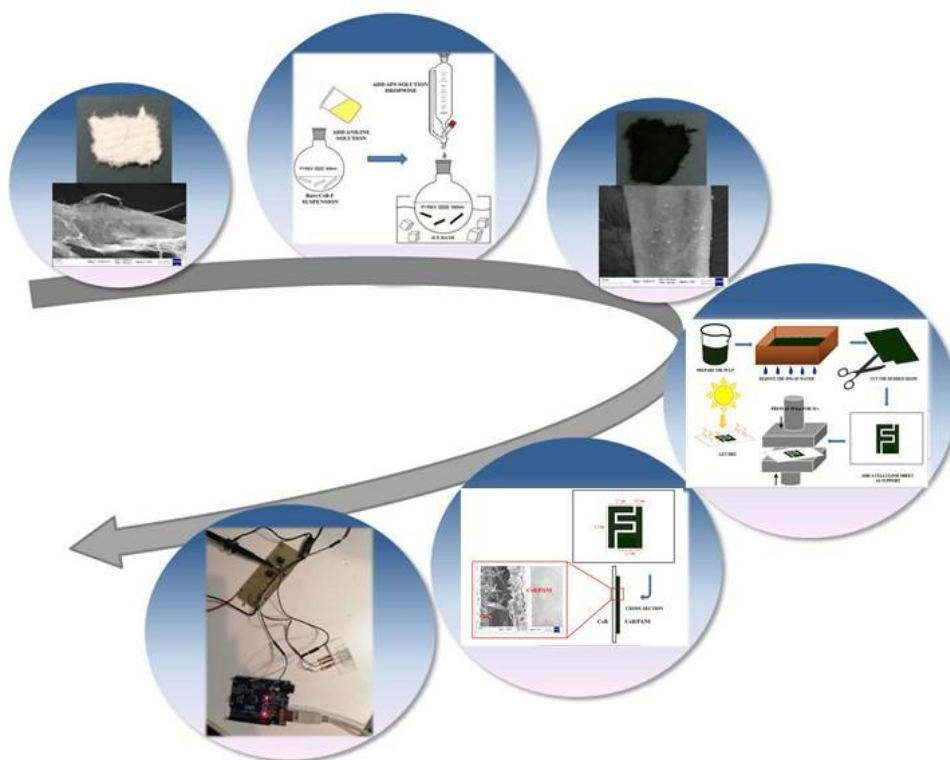
Scheme 1. Preparation steps for Cell/PANI-F.

4.3 Preparation of Cell/PANI-S

10 g of Cell/PANI-F were added to 1.0 L of an acid solution (ca. pH 3.0, 25 wt% $\text{Al}_2(\text{SO}_4)_3$ in demineralized water) and stirred for 5 min. The fibers were partially dried in a square sieve (21.0 cm x 14.8 cm size). The sheet was pressed at 50 bar pressure (P50 AXA manual hydraulic press) for 10 s to obtain the Cell/PANI-S (200 gsm, 0.40 mm thickness). Similarly, a 1.25 mm thick sheet was prepared by using 30 g of fibres (see Scheme S1 for the industrial steps details).

4.4 Preparation of Cell/PANI-TS

The wet coupling method employed in the paper industry to produce sheets of paper with variable thicknesses or with greater resistance was used to prepare the Cell/PANI-TS samples. A Cell/PANI-S of 0.40 mm thickness was cut in the desired shape and coupled with a cellulose sheet (th. 0.40 mm) moistened with water. The two sheets were then pressed (50 bar, 10 s) and dried at 80 °C for 10 min. The electrical connections were made afterwards with copper adhesive tape and silver glue, see Scheme S2 for details. The whole six-steps preparation from fibers to touch sensor is reported in Scheme 2.



Scheme 2. Six-steps preparation for cellulose/PANI touch sensor preparation.

4.5 Instruments

ATR-FTIR analyses were performed using a Perkin Elmer Spectrum Two spectrophotometer, equipped with a Universal ATR accessory, with a resolution of 0.5 cm^{-1} in the range $4000\text{--}400\text{ cm}^{-1}$. The samples were directly analyzed performing 40 scans for any analysis.

The determination of PANI amount in Cell/PANI-F was performed with an automatic Kjeldahl Nitrogen Analyzer (Gerhardt Bonn). The Kjeldahl analysis was carried out on four Cell/PANI-F samples and a blank sample (cellulose bare fibre treated exactly as the Cell/PANI-F) using the following protocol. 1.0 g of each sample was put in a glass weighing flask and placed in a Kjeldahl test tube. A catalyst tablet (1 tablet contains 3.5 g of K_2SO_4 and 3.5 mg of Se) (Kjeldahl tablets, 1.18649 Supelco, Merck), 20 mL of concentrated H_2SO_4 (sulfuric acid 95-98%, ACS reagent,

258105 Sigma-Aldrich) and 4 glass spheres were then added. The test tubes were heated to 350 ° C for 5 h. The final solution must be clear and colourless. Finally, the test tubes were inserted in the Kjeldahl titration instrument and the potentiometric titration automatically start with 0.100 M HCl in presence of an acid basic indicator (a mixture of methyl red and bromocresol green).

SEM images were recorded at 25 kV with a Sem Zeiss EVO 50 EP equipped with Oxford INCA 350; EDS Spectrometer equipped with a Bruker Z200 energy dispersive microanalysis (EDX) system was used for semi-quantitative chemical analysis and mapping.

4.6 Electrical measurements

Cell/PANI-S resistance was measured with a keysight B2902A source meter units in a 4-line-probe configuration by exploiting a home-made holder that is composed by 4 parallel copper electrodes on a glass slide (Figure S1). The sample was prepared with a rectangular shape and was held down with an insulating material by exerting a uniform pressure on all the surface. The inner electrodes measure the difference of potential while a constant current flow was forced between the two outer electrodes. The measurements were performed at different current values (100, 200, 300 μ A) and a line passing from the origin was always obtained. The resistance (R) was calculated with the Ohm's law and the sheet resistance (R_{\square}) is equal to:

$$R_{\square} = R \frac{W}{L}$$

Where W and L are the width and the length, respectively.

The specific resistance (ρ) can be calculated by:

$$\rho = R_{\square} t$$

Where t is the thickness. The specific conductance (κ) is calculated by:

$$\kappa = \frac{1}{\rho}$$

299 **4.7 Test execution for capacitive vs pressure curves**

300 In order to standardize the measurements, a nitrile rubber (Buna-N, Perbunan - NBR) was chosen as
301 dielectric material and was interposed between the pressure generator and the sensor (P.Cataldi et al.,
302 2018). The sensor was housed in the appropriate seat apparatus reported in Figure S4 and a force-
303 weight was exerted with an increase step of 1.0 g (subsequently converted into Pascal) on the whole
304 sensor surface and the capacity was recorded at the same time.

305

306 **ASSOCIATED CONTENT**

307 **Supporting information**

308 The Supporting Information is available free of charge on the Publication website at DOI:

309 **AUTHOR INFORMATION**

310 **Corresponding Autors**

311 ***Barbara Ballarin**, Dipartimento di Chimica Industriale Toso Montanari, UNIBO, Viale
312 Risorgimento 4, 40136 Bologna-IT
313 orcid.org/0000-0003-3698-2352; E-mail: barbara.ballarin@unibo.it

314 ***Isacco Gualandi**, Dipartimento di Chimica Industriale Toso Montanari, UNIBO, Viale
315 Risorgimento 4, 40136 Bologna-IT
316 orcid.org/0000-0002-6823-7501; E-mail: isacco.gualandi2@unibo.it

317

318

319 **Author contributions**

320 B.B., E.S., I.G., I.R., conceived the project, supervised the preparation and analysis of the samples,
321 analysed the data and wrote the paper. C.P. designed and developed the electronic experiments set-
322 up. S.S. helped to assemble the sheets and the touch sensors. M.C.C. and F.G. participated in
323 analytical data collection and analysis. D.T. and D.N. revised the manuscript.

324 ACKNOWLEDGEMENTS

325 The authors thank the University of Bologna for financial support. The authors gratefully thank Dr.
326 Sandra Stipa and Dr. Fabrizio Tarterini for the SEM images and Kjeldahl analyses. Finally the authors
327 especially thank Cromatos s.r.l. and Roberto Bezzi for the sheets preparation.

328

329 REFERENCES

- 330 10° Corso di Tecnologia per Tecnici Cartari, edizione 2002/2003; Scuola Interregionale di
331 Tecnologia per Tecnici Cartari, Via Don G. Minzoni, 50 - 37138 Verona
- 332 Aguado, R., Murtinho, D., & Valente, A. J. M. (2019). A broad overview on innovative
333 functionalized paper solutions. *Nordic Pulp and Paper Research Journal*, 34(4), 395–416.
334 <https://doi.org/10.1515/npprj-2019-0036>
- 335 Baptista, A. C., Ropio, I., Romba, B., Nobre, J. P., Henriques, C., Silva, J. C., Ferreira, I. (2018).
336 Cellulose-based electrospun fibers functionalized with polypyrrole and polyaniline for fully
337 organic batteries. *Journal of Material Chemistry A*, 6(1), 256–265.
338 <https://doi.org/10.1039/c7ta06457h>
- 339 Cataldi, P.; Dussoni, S.; Ceseracciu, L.; Maggiali, M.; Natale, L.; Metta, G.; Athanassiou, A.;
340 Bayer, I. S. (2018) Carbon nanofiber versus graphene-based stretchable capacitive touch
341 sensors for artificial electronic skin, *Advanced Science*, 5, 1700587-1700597.
- 342 Cases, F., Huerta, F., Garcés, P., Morallón, E., & Vázquez, J. L. (2001). Voltammetric and in situ
343 FTIRS study of the electrochemical oxidation of aniline from aqueous solutions buffered at pH
344 5. *Journal of Electroanalytical Chemistry*, 501(1–2), 186–192. <https://doi.org/10.1016/S0022->

0728(00)00526-X

Chougale, U. M., Thombare, J. V., Fulari, V. J., & Kadam, A. B. (2013). Synthesis of polyaniline nanofibres by SILAR method for supercapacitor application. *2013 International Conference on Energy Efficient Technologies for Sustainability, ICEETS 2013*, (April), 1078–1083. <https://doi.org/10.1109/ICEETS.2013.6533537>

Cromatos s.r.l. is an industrial group operating worldwide dedicated to the production, formulation and marketing of dyes, pigments and chemical products for industry. (<https://www.cromatos.com>).

Das, P., Mai, V. C., & Duan, H. (2019). Flexible bioinspired ternary nanocomposites based on carboxymethyl cellulose/nanoclay/graphene oxide. *ACS Applied Polymer Materials*, 1(6), 1505–1513. research-article. <https://doi.org/10.1021/acsapm.9b00245>

Dhibar, S., & Das, C. K. (2014). Silver nanoparticles decorated polyaniline/multiwalled carbon nanotubes nanocomposite for high-performance supercapacitor electrode. *Industrial and Engineering Chemistry Research*, 53(9), 3495–3508. <https://doi.org/10.1021/ie402161e>

Gao, W., Ota, H., Kiriya, D., Takei, K., & Javey, A. (2019). Flexible Electronics toward Wearable Sensing. *Accounts of Chemical Research*, 52(3), 523–533. <https://doi.org/10.1021/acs.accounts.8b00500>

Gu, Y., & Huang, J. (2013). Colorimetric detection of gaseous ammonia by polyaniline nanocoating of natural cellulose substances. *Colloids and Surfaces A: Physicochemical and Engineering Aspects*, 433, 166–172. <https://doi.org/10.1016/j.colsurfa.2013.05.016>

John, A., Mahadeva, S. K., & Kim, J. (2010). The preparation, characterization and actuation behavior of polyaniline and cellulose blended electro-active paper. *Smart Materials and Structures*, 19(4). <https://doi.org/10.1088/0964-1726/19/4/045011>

Kanaparthi, S., & Badhulika, S. (2017). Low cost, flexible and biodegradable touch sensor fabricated by solvent-free processing of graphite on cellulose paper. *Sensors and Actuators, B: Chemical*, 242, 857–864. <https://doi.org/10.1016/j.snb.2016.09.172>

371 Ke, S., Ouyang, T., Zhang, K., Nong, Y., Mo, Y., Mo, Q., Cheng, F. (2019). Highly conductive
 372 cellulose network/polyaniline composites prepared by wood fractionation and in situ
 373 polymerization of aniline. *Macromolecular Materials and Engineering*, 304(7), 1–10.
 374 <https://doi.org/10.1002/mame.201900112>

375 Khan, A., Abas, Z., Kim, H. S., & Kim, J. (2016). Recent progress on cellulose-based electro-active
 376 paper, its hybrid nanocomposites and applications. *Sensors (Switzerland)*, 16(8), 1–30.
 377 <https://doi.org/10.3390/s16081172>

378 Liu, X. X., Zhang, L., Li, Y. B., Bian, L. J., Su, Z., & Zhang, L. J. (2005). Electropolymerization of
 379 aniline in aqueous solutions at pH 2 to 12. *Journal of Materials Science*, 40(17), 4511–4515.
 380 <https://doi.org/10.1007/s10853-005-0854-x>

381 Luo, Y., & Huang, J. (2014). Surface modification of natural cellulose substances: Toward
 382 functional materials and applications. *Science China Chemistry*, 57(12), 1672–1682.
 383 <https://doi.org/10.1007/s11426-014-5226-4>

384 Ma, Z., Wang, W., & Yu, D. (2020). Assembled wearable mechanical sensor prepared based on
 385 cotton fabric. *Journal of Materials Science*, 55(2), 796–805. [https://doi.org/10.1007/s10853-](https://doi.org/10.1007/s10853-019-04035-0)
 386 [019-04035-0](https://doi.org/10.1007/s10853-019-04035-0)

387 Masood, A., Shoukat, Z., Yousaf, Z., Sana, M., Faisal Iqbal, M., Rehman, A. R., Razaq, A. (2019).
 388 High capacity natural fiber coated conductive and electroactive composite papers electrode for
 389 energy storage applications. *Journal of Applied Polymer Science*, 136(13), 1–6.
 390 <https://doi.org/10.1002/app.47282>

391 Ngamna, O., Morrin, A., Killard, A. J., Moulton, S. E., Smyth, M. R., & Wallace, G. G. (2007).
 392 Inkjet printable polyaniline nanoformulations. *Langmuir*, 23(16), 8569–8574.
 393 <https://doi.org/10.1021/la700540g>

394 Pang, Z., Yang, Z., Chen, Y., Zhang, J., Wang, Q., Huang, F., & Wei, Q. (2016). A room
 395 temperature ammonia gas sensor based on cellulose/TiO₂/PANI composite nanofibers.
 396 *Colloids and Surfaces A: Physicochemical and Engineering Aspects*, 494, 248–255.

397 <https://doi.org/10.1016/j.colsurfa.2016.01.024>

398 Rafatmah, E., & Hemmateenejad, B. (2020). Dendrite gold nanostructures electrodeposited on
 399 paper fibers: Application to electrochemical non-enzymatic determination of glucose. *Sensors*
 400 *and Actuators, B: Chemical*, 304(October 2019), 127335.
 401 <https://doi.org/10.1016/j.snb.2019.127335>

402 Razak S. I. A, Sharif, N. H. M. N. (2014). Elect rically Conductive Paper of Polyaniline Modified
 403 Pineapple Leaf Fiber. *Fibers and Polymers*, 15, 1107. [https://doi.org/10.1007/s12221-014-](https://doi.org/10.1007/s12221-014-1107-x)
 404 1107-x

405 Report EU. (n.d.). Retrieved from [https://www.unenvironment.org/news-and-stories/press-](https://www.unenvironment.org/news-and-stories/press-release/un-report-time-seize-opportunity-tackle-challenge-e-waste)
 406 release/un-report-time-seize-opportunity-tackle-challenge-e-waste

407 Sanandiya, N. D., Vijay, Y., Dimopoulou, M., Dritsas, S., & Fernandez, J. G. (2018). Large-scale
 408 additive manufacturing with bioinspired cellulosic materials. *Scientific Reports*, 8(1), 1–8.
 409 <https://doi.org/10.1038/s41598-018-26985-2>

410 Shao, Q., Niu, Z., Hirtz, M., Jiang, L., Liu, Y., Wang, Z., & Chen, X. (2014). High-performance
 411 and tailorable pressure sensor based on ultrathin conductive polymer film. *Small*, 10(8), 1466–
 412 1472. <https://doi.org/10.1002/sml.201303601>

413 Sharifi, H., Zabihzadeh, M., & Ghorbani, M. (2018). The application of response surface
 414 methodology on the synthesis of conductive polyaniline/cellulosic fiber nanocomposites.
 415 *Carbohydrate Polymers*, 194(February), 384–394.
 416 <https://doi.org/10.1016/j.carbpol.2018.04.083>

417 Sharma, K., Pareek, K., Rohan, R., & Kumar, P. (2019). Flexible supercapacitor based on three-
 418 dimensional cellulose/graphite/polyaniline composite. *International Journal of Energy*
 419 *Research*, 43(1), 604–611. <https://doi.org/10.1002/er.4277>

420 Shoaie, N., Daneshpour, M., Azimzadeh, M., Mahshid, S., Khoshfetrat, S. M., Jahanpeyma, F., ...
 421 Foruzandeh, M. (2019). Electrochemical sensors and biosensors based on the use of
 422 polyaniline and its nanocomposites: a review on recent advances. *Microchimica Acta*, 186(7).

423 <https://doi.org/10.1007/s00604-019-3588-1>

424 Silva, L. E., Cunha Claro, P. I., Sanfelice, R. C., Guimarães, M., de Oliveira, J. E., Ugucioni, J. C.,
 425 Denzin Tonoli, G. H. (2019). Cellulose nanofibrils modification with polyaniline aiming at
 426 enhancing electrical properties for application in flexible electronics. *Cellulose Chemistry and*
 427 *Technology*, 53(7–8), 775–786. <https://doi.org/10.35812/CelluloseChemTechnol.2019.53.76>

428 Singh, P., & Shukla, S. K. (2020). Advances in polyaniline-based nanocomposites. *Journal of*
 429 *Materials Science*, 55(4), 1331–1365. <https://doi.org/10.1007/s10853-019-04141-z>

430 Tanguy, N. R., Thompson, M., & Yan, N. (2018). A review on advances in application of
 431 polyaniline for ammonia detection. *Sensors and Actuators, B: Chemical*, 257, 1044–1064.
 432 <https://doi.org/10.1016/j.snb.2017.11.008>

433 Tao, L. Q., Zhang, K. N., Tian, H., Liu, Y., Wang, D. Y., Chen, Y. Q., Ren, T. L. (2017). Graphene-
 434 Paper Pressure Sensor for Detecting Human Motions. *ACS Nano*, 11(9), 8790–8795.
 435 <https://doi.org/10.1021/acsnano.7b02826>

436 Teo, M. Y., Stuart, L., Devaraj, H., Liu, C. Y., Aw, K. C., & Stringer, J. (2019). The: In situ
 437 synthesis of conductive polyaniline patterns using micro-reactive inkjet printing. *Journal of*
 438 *Materials Chemistry C*, 7(8), 2219–2224. <https://doi.org/10.1039/c8tc06485g>

439 Tian, Y., Qu, K., & Zeng, X. (2017). Investigation into the ring-substituted polyanilines and their
 440 application for the detection and adsorption of sulfur dioxide. *Sensors and Actuators, B:*
 441 *Chemical*, 249, 423–430. <https://doi.org/10.1016/j.snb.2017.04.057>

442 Tobjörk, D., & Österbacka, R. (2011). Paper electronics. *Advanced Materials*, 23(17), 1935–1961.
 443 <https://doi.org/10.1002/adma.201004692>

444 Wang, Q., Sun, J., Yao, Q., Ji, C., Liu, J., & Zhu, Q. (2018). 3D printing with cellulose materials.
 445 *Cellulose*, 25(8), 4275–4301. <https://doi.org/10.1007/s10570-018-1888-y>

446 Wang, Yanhu, Zhang, L., Zhao, P., Ge, S., Yan, M., & Yu, J. (2019). Visual distance readout to
 447 display the level of energy generation in paper-based biofuel cells: application to enzymatic
 448 sensing of glucose. *Microchimica Acta*, 186(5). <https://doi.org/10.1007/s00604-019-3374-0>

449 Wang, Yanmin, Liu, A., Han, Y., & Li, T. (2019). Sensors based on conductive polymers and their
 450 composites: a review. *Polymer International*, (September 2019).
 451 <https://doi.org/10.1002/pi.5907>

452 Yan, H., Guo, Y., Lai, S., Sun, X., Niu, Z., & Wan, P. (2016). Flexible Room-Temperature Gas
 453 Sensors of Nanocomposite Network-Coated Papers. *ChemistrySelect*, 1(11), 2816–2820.
 454 <https://doi.org/10.1002/slct.201600648>

455 Youssef, A. M., El-Samahy, M. A., & Abdel Rehim, M. H. (2012). Preparation of conductive paper
 456 composites based on natural cellulosic fibers for packaging applications. *Carbohydrate*
 457 *Polymers*, 89(4), 1027–1032. <https://doi.org/10.1016/j.carbpol.2012.03.044>

458 Yu, Z., Tang, Y., Cai, G., Ren, R., & Tang, D. (2019). Paper Electrode-Based Flexible Pressure
 459 Sensor for Point-of-Care Immunoassay with Digital Multimeter. *Analytical Chemistry*, 91(2),
 460 1222–1226. <https://doi.org/10.1021/acs.analchem.8b04635>

461 Zang, X., Jiang, Y., Wang, X., Wang, X., Ji, J., & Xue, M. (2018). Highly sensitive pressure
 462 sensors based on conducting polymer-coated paper. *Sensors and Actuators, B: Chemical*,
 463 273(July), 1195–1201. <https://doi.org/10.1016/j.snb.2018.06.132>

464 Zhang, W., Wu, Z., Hu, J., Cao, Y., Guo, J., Long, M., ... Jia, D. (2019). Flexible chemiresistive
 465 sensor of polyaniline coated filter paper prepared by spraying for fast and non-contact
 466 detection of nitroaromatic explosives. *Sensors and Actuators B: Chemical*, 127233.
 467 <https://doi.org/10.1016/j.snb.2019.127233>

468 Zhang, Y., Yang, Z., Yu, Y., Wen, B., Liu, Y., & Qiu, M. (2019). Tunable electromagnetic
 469 interference shielding ability in a one-dimensional bagasse fiber/polyaniline heterostructure.
 470 *ACS Applied Polymer Materials*, 1(4), 737–745. <https://doi.org/10.1021/acsapm.8b00025>

471